Progress In Electromagnetics Research Letters, Vol. 88, 75–81, 2020

A Novel Lumped LC Resonator Antenna with Air-Substrate for 5G Mobile Terminals

Shahanawaz Kamal[1, *], Abdullahi SB Mohammed[1], Mohd Fadzil Bin Ain[1], Fathul Najmi[1], Roslina Hussin[1], Zainal Arifin Ahmad[2], Ubaid Ullah[3], Mohamadariff Othman[4], and Mohd Fariz Ab Rahman[5]

Abstract—The extending applications for mobile computing have experienced immense progress over the previous decade. However, this has ultimately influenced the shortage of bandwidth. Therefore, to fulfill the consumers' demand, inexpensive antennas need to be uniquely designed for the next/fifth generation (5G) frequency spectrum. Consequently, this paper presents a novel antenna composed of inductors (L) or capacitors (C) on an air-substrate. Zinc (Zn) and copper (Cu) materials are utilized to fabricate the lumped LC resonator prototype. The effects of antenna's and substrate's thickness on resonant frequency or bandwidth have been studied. The finalized configuration engaged 1113 sq. mm area and operated at 28 GHz with approximately 3 GHz bandwidth. At resonant frequency, the system demonstrates peak gain and efficiency values of 10.6 dBi and 91%, respectively. The core objective of this paper is to report an antenna featuring simple and economical design along with premium results for 5G mobile terminals.

1. INTRODUCTION

Recent expansions in the handheld devices have fostered an augmenting need for the development of cost-effective radiating elements with improved bandwidth [1, 2]. Conventional printed antenna systems possess many fascinating characteristics, but they suffer from a fundamental shortcoming of narrow bandwidth [3, 4]. This ultimately outlines a genuine challenge for engineers to achieve the broadband necessities of modern communication devices.

Several bandwidth improvement procedures have been reported in the literature. Matin et al. [5] and Croq and Papiernik [6] described one method of mounting parasitic elements over the main radiating patch, whereas Huynh and Lee. [7] reported another method which introduced slots in the antenna. However, these approaches proved effective at the cost of an increased profile. In order to triumph wideband operation with compact outline Xiao et al. [8] excited the antenna's TM10 and TM01 modes simultaneously. Likewise, several other authors were successful in getting an impedance bandwidth above 12% by experimenting with the resonant modes [9–13]. It is evident from the results presented in [14, 15] that with a proper feeding arrangement, the operating bandwidth can be extended above 28%. Nevertheless, this scheme is inappropriate for execution in an electrically thin substrate. Introducing reactive impedance surface characterizes one more method [16, 17]. Among all these techniques, increasing the substrate's thickness is one of the most conventional ones [18]. However, this practice is counterproductive because of the indication of the surface waves, which

Received 5 September 2019, Accepted 19 November 2019, Scheduled 10 December 2019

* Corresponding author: Shahanawaz Kamal (shahanawazkamal@gmail.com).

[1] School of Electrical and Electronic Engineering, Universiti Sains Malaysia, Nibong Tebal 14300, Malaysia. [2] School of Materials and Mineral Resources Engineering, Universiti Sains Malaysia, Nibong Tebal 14300, Malaysia. [3] Networks and Communication Engineering Department, Al Ain University of Science and Technology, Abu Dhabi 112612, United Arab Emirates. [4] Department of Electrical Engineering, University of Malaya, Kuala Lumpur 50603, Malaysia. [5] Faculty of Bioengineering and Technology, Universiti Malaysia Kelantan - Jeli Campus, Jeli 17600, Malaysia.

ultimately results into spurious coupling and poor efficiency. Then again, this inadequacy can be eliminated by replacing thicker substrates with a low permittivity material for instance air and the like. Furthermore, an enhanced antenna bandwidth can be accomplished by electromagnetic band gap structures [19–21]. Significantly, the fifth generation of mobile communications is anticipated to be a meaningful enhancement on the preceding networks by presenting superior bandwidth and other considerations [22, 23]. Consequently, this paper presents a network of inductors and capacitors as the main resonating element with remarkable bandwidth for 28 GHz mobile terminals. The lumped LC resonator antenna was designed such that the operating frequency can be tuned by adjusting the number, length, and width of fingers. Considering the high electrical conductivity property in addition to human body adaptation factors, Cu and Zn were selected as radiating materials in this study [24]. In order to reduce the cost of fabrication significantly, the air-substrate was incorporated in the design. Table 1 summarizes the results of the antenna.

Table 1. Performance of the proposed lumped LC resonator antenna.

Size (mm^2)	Resonant Frequency (GHz)	Gain (dBi)	Directivity Gain (dBi)	Return Loss (dB)	Bandwidth (GHz)	Efficiency (%)	Impedance (Ohm)	
							Real	Imaginary
53 × 21	28	10.6	11.7	−29.898	3.321	91	50	0

2. DESIGN, CONFIGURATION AND ANALYTICAL MODEL

The antenna contains passive components including a set of inductors and capacitors (Fig. 1). The lumped LC resonator prototype, designed in ADS software [25], consists of top (resonator) and bottom (ground) layers (Fig. 2). These layers were separated by an air-substrate of 1 mm thickness having a dielectric constant (ϵ_r) of 1.00059. Two coaxial-fed antennas were fabricated by employing Zn and Cu of 1 mm thickness. The developed system is suitable for modern compact devices as it occupies an area of only 5 lambda × 2 lambda.

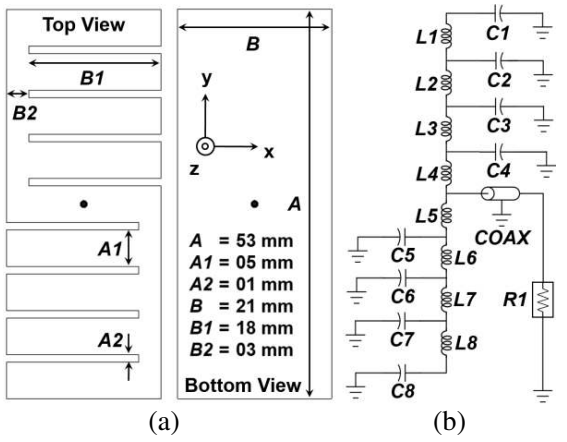

Figure 1. The antenna's (a) geometry and (b) equivalent circuit.

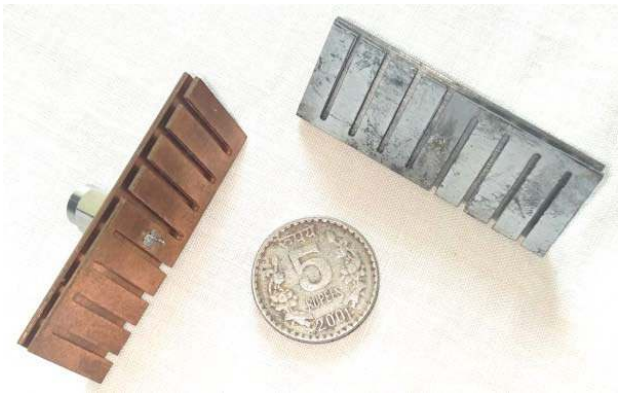

Figure 2. The fabricated lumped LC resonator antennas (left: Cu and right: Zn).

Inductors were typically outlined to function as conductors. The multiple strips with meandered edges were fashioned to control their magnetic fields and magnitude. Furthermore, these inductors were shorted across the capacitors to facilitate equal currents at the end of every finger which ultimately decided capacitance values. The values of inductance (L) and capacitance (C) can be calculated using

the following equations [26, 27],

$$L = 200 \times 10^{-9} B1 \left[\ln \left(\frac{2B1}{A1 + t} \right) + \left(0.50049 + \frac{A1}{3B1} \right) \right] \tag{1}$$

$$C = (\varepsilon_r + 1) B1 \left[(N - 3) X1 + X2 \right] \tag{2}$$

where t is the conductor thickness, ε_r the dielectric constant of the substrate, N the number of fingers, and $X1$ and $X2$ are the capacitance per unit length of the fingers and can be estimated from the subsequent equations,

$$X1 = 4.409 \tanh \left[0.55 \left(\frac{h}{A2} \right)^{0.45} \right] \times 10^{-6} \tag{3}$$

$$X2 = 9.920 \tanh \left[0.52 \left(\frac{h}{A2} \right)^{0.50} \right] \times 10^{-6} \tag{4}$$

where h is the substrate thickness.

The total series capacitance of a capacitor can also be articulated by [28],

$$C = 2\varepsilon_0 \varepsilon_{eff} \frac{K(k)}{K(k')} (N - 1) B1 \tag{5}$$

where ε_0 is the permittivity of free space, and ε_{eff} is the effective dielectric constant of the transmission line of width (w) and can be accomplished by,

$$\varepsilon_{eff} = \frac{\varepsilon_r + 1}{2} + \frac{\varepsilon_r - 1}{2} \left(1 + \frac{10h}{w} \right)^{-0.5} \tag{6}$$

Moreover, the ratio of complete elliptic integral of first kind $K(k)$ and its complement $K(k')$ is given by the following equations,

$$\frac{K(k)}{K(k')} = \frac{1}{\pi} \ln \left[2 \left(\frac{1 + \sqrt{k}}{1 - \sqrt{k}} \right) \right] \quad \text{for} \quad 0.707 \leq k \leq 1 \tag{7}$$

$$\frac{K(k)}{K(k')} = \frac{\pi}{\ln \left[2 \left(\frac{1 + \sqrt{k'}}{1 - \sqrt{k'}} \right) \right]} \quad \text{for} \quad 0 \leq k \leq 0.707 \tag{8}$$

$$\text{where,} \quad k = \tan^2 \left(\left(\frac{\pi}{4} \right) \left(\frac{A2}{A1 + A2} \right) \right) \quad \text{and} \quad k' = \sqrt{1 - k^2} \tag{9}$$

The resonant frequency (f) and impedance (Z_0) of the coaxial feed can be achieved from the successive equations,

$$f = \frac{1}{2\pi \sqrt{LC}} \tag{10}$$

$$Z_0 = \frac{120\pi}{\sqrt{\varepsilon_{eff} \left[\left(\frac{w}{h} \right) + 1.393 + 0.667 \ln \left(\left(\frac{w}{h} \right) + 1.4444 \right) \right]}} \tag{11}$$

3. RESULTS AND DISCUSSION

3.1. Return Loss

The performance of the lumped LC resonator antenna system was analyzed by focusing on three classes (A, B, and C) that we have defined. CST software [29] was utilized to obtain the optimized results. For a Class-A Antenna, the thickness of the substrate was considered as 1.00 mm, and the total board area of all the layers was selected as 1113 mm^2. However, parametric simulation studies were carried

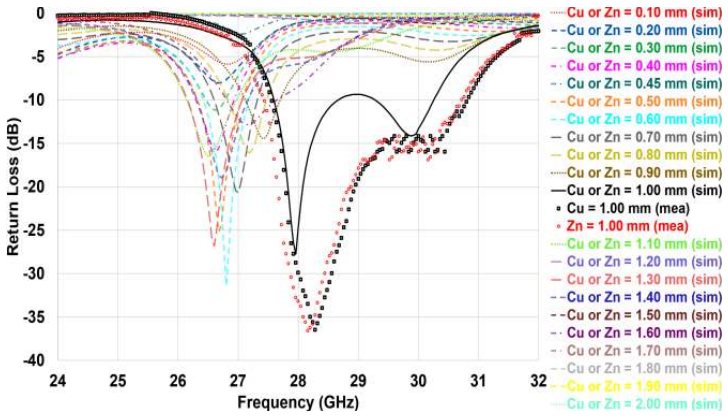

Figure 3. Simulated and measured return loss of the lumped LC resonator antenna.

out for deciding the height of the resonator and the ground. Twenty-one different sizes were considered for investigation notably 0.10 mm, 0.20 mm, 0.30 mm, 0.40 mm, 0.45 mm, 0.50 mm, 0.60 mm, 0.70 mm, 0.80 mm, 0.90 mm, 1.00 mm, 1.10 mm, 1.20 mm, 1.30 mm, 1.40 mm, 1.50 mm, 1.60 mm, 1.70 mm, 1.80 mm, 1.90 mm, and 2.00 mm (Fig. 3). Among all these cases, the arrangement with 1.00 mm thickness showed return loss value of −29.898 dB at 28 GHz and covered the frequencies of 27.519 GHz to 30.840 GHz. Moreover, precisely comparable results were obtained for both Cu and Zn materials.

For a Class-B Antenna, the total size (53 mm × 21 mm) and height (1.00 mm) of the resonator or ground were kept constant, while the thickness of the substrate was allowed to vary. Twenty distinct sizes including 0.10 mm, 0.20 mm, 0.30 mm, 0.40 mm, 0.50 mm, 0.60 mm, 0.70 mm, 0.80 mm 0.90 mm, 1.00 mm, 1.10 mm, 1.20 mm, 1.30 mm, 1.40, 1.50, 1.60, 1.70 mm, 1.80 mm, 1.90 mm, and 2.00 mm were considered (Fig. 4). Since each finger was instituted in the resonator of Class A and B Antennas, the overall capacitance in the system decreased, even though the mutual capacitance in each finger increased.

For a Class-C Antenna, the height of the substrate, resonator, and ground were fixed, whilst the number of fingers was extended from one to eight (Fig. 5). A rise in the total inductance was witnessed with an increase in the wire's length. Although adding fingers confirmed a comparable effect on the overall capacitance as expressed for Class A and B Antennas, the growth in inductance dominated. Therefore, the resonant frequency decreased with an increase in the number of fingers.

The simulated Smith chart obtained from the equivalent circuit model and the measured results are presented in Fig. 6. It is evident from the results illustrated in Figs. 3 to 6 that the desired resonance of 28 GHz could be accomplished when and Cu or Zn = Air = 1.00 mm and $N = 8$. Consequently, these dimensions were preferred for fabrication. The measurements of the constructed systems were conducted using Agilent's N5245A PNA-X Microwave Network Analyzer.

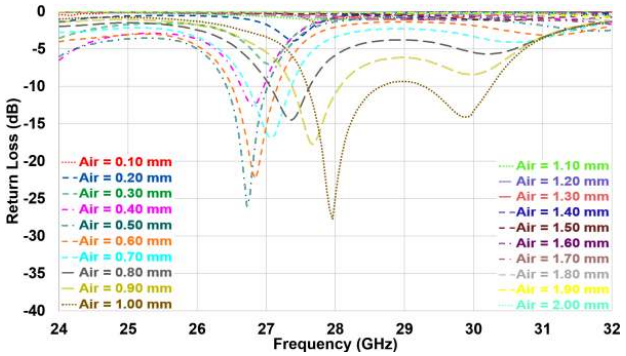

Figure 4. Parametric simulation studies for the design of substrate.

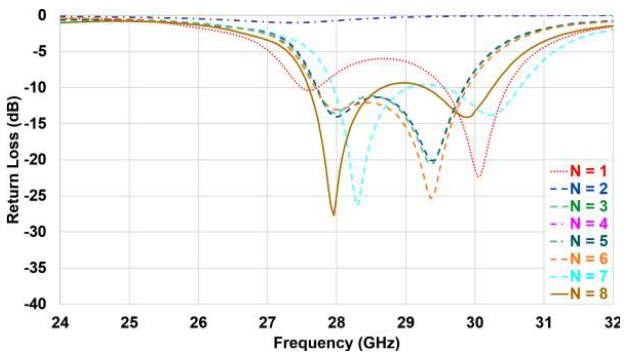

Figure 5. Simulated return loss with variation in the number of fingers.

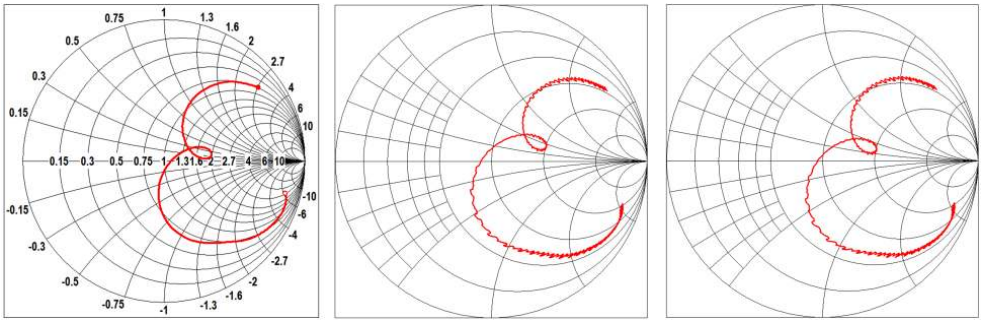

(a) (b) (c)

Figure 6. (a) Simulated smith chart obtained from the equivalent circuit and measured results for (b) Cu or (c) Zn.

3.2. Surface Current Distribution

The vector field and current distribution of the finalized configuration is demonstrated in Fig. 7. The charge distribution at the resonator and ground planes were produced by exciting them with a coaxial feed probe. This ultimately transformed the TEM mode across the probe aperture into the parallel plate mode. Therefore, the higher-order mode's evanescent waves were confined in the vicinity of the probe, whereas the zero-order parallel plate mode propagated away to excite the TM10 resonant mode of the antenna. Additionally, the positive and negative field distributions produced due to the feed effect was comparable to a printed patch antenna. The repulsive force between these positive charges were accountable for producing a charge density ($J\left(x', y'\right)$) around the edges,

$$J\left(x', y'\right) = \frac{2}{\pi A1}\sqrt{1-\left(\frac{2x'}{A1}\right)^2}\sum_{j=0}^{N} I\left(i,j\right), \quad -\frac{A}{2} \le x \le \frac{A}{2} \tag{12}$$

where $I\left(i,j\right) = \begin{cases} I_0 \; for j = 0 \\ \frac{I_0}{2n} \; otherwise \end{cases}$. Consequently, the fringing fields caused by these charges resulted in radiation.

3.3. Radiation Pattern

Figure 8 shows the simulated and measured radiation patterns of the lumped LC resonator antenna at 28 GHz. The total field amplitude combining E_θ and E_φ components was measured at the Anechoic Chamber, Universiti Sains Malaysia. The radiation patterns of E or H plane are nearly omnidirectional.

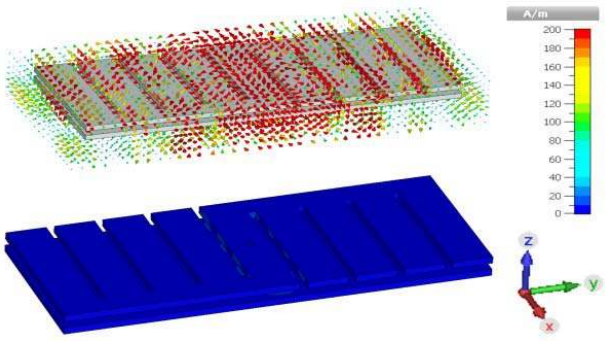

Figure 7. The vector field (top) and current distribution (bottom) of the antenna.

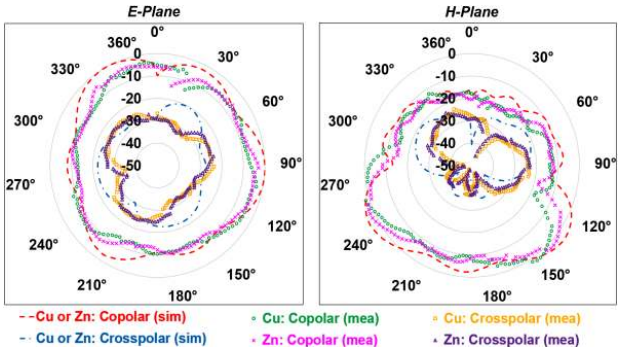

Figure 8. Simulated and measured radiation pattern of the lumped LC resonator antenna.

At resonant frequency, the system showed a peak gain and efficiency values of 10.6 dBi and 91%, respectively.

4. CONCLUSION

An innovative outline of the lumped LC resonator antenna was designed to operate at 5G band (28 GHz). The proposed system involved a network of inductors and capacitors short-circuited to the ground. The antenna's operating frequency was tuned by varying the thickness of the resonator, ground, and substrate. The radiating elements were engineered on an air-substrate which reduced the fabrication cost significantly. In addition, the finalized design occupied a small volume and demonstrated appropriateness for integration with modern miniature devices. The antenna was tested in the laboratory which exhibited good agreement concerning simulation and measurement outcomes.

ACKNOWLEDGMENT

This work was supported by the Universiti Sains Malaysia under Grant RUINO.1001/PELECT/8014009 and Ministry of Higher Education under Fundamental Research Grant Scheme 203.PELECT.6071429.

REFERENCES

1. Ban, Y.-L., et al., "4G/5G multiple antennas for future multi-mode smartphone applications," *IEEE Access*, Vol. 4, 2981–2988, 2016.
2. Zeng, Y. and R. Zhang, "Cost-effective millimeter-wave communications with lens antenna array," *IEEE Wireless Communications*, Vol. 24, 81–87, 2017.
3. Wang, Y., et al., "5G mobile: Spectrum broadening to higher-frequency bands to support high data rates," *IEEE Vehicular Technology Magazine*, Vol. 9, No. 3, 39–46, 2014.
4. Balanis, C. A., *Modern Antenna Handbook*, John Wiley & Sons, 2011.
5. Matin, M., B. Sharif, and C. Tsimenidis, "Dual layer stacked rectangular microstrip patch antenna for ultra wideband applications," *IET Microwaves, Antennas & Propagation*, Vol. 1, 1192–1196, 2007.
6. Croq, F. and A. Papiernik, "Stacked slot-coupled printed antenna," *IEEE Microwave and Guided Wave Letters*, Vol. 1, 288–290, 1991.
7. Huynh, T. and K.-F. Lee, "Single-layer single-patch wideband microstrip antenna," *Electronics Letters*, Vol. 31, 1310–1312, 1995.
8. Xiao, S., B.-Z. Wang, W. Shao, and Y. Zhang, "Bandwidth-Enhancing Ultralow-Profile Compact Patch Antenna," *IEEE Transactions on Antennas and Propagation*, Vol. 53, 3443–3447, 2005.
9. Lu, W.-J., Q. Li, S.-G. Wang, and L. Zhu, "Design approach to a novel dual-mode wideband circular sector patch antenna," *IEEE Transactions on Antennas and Propagation*, Vol. 65, 4980–4990, 2017.
10. Liu, N.-W., L. Zhu, W.-W. Choi, and X. Zhang, "A low-profile aperture-coupled microstrip antenna with enhanced bandwidth under dual resonance," *IEEE Transactions on Antennas and Propagation*, Vol. 65, 1055–1062, 2017.
11. Liu, J., Q. Xue, H. Wong, H. W. Lai, and Y. Long, "Design and analysis of a low-profile and broadband microstrip monopolar patch antenna," *IEEE Transactions on Antennas and Propagation*, Vol. 61, 11–18, 2013.
12. Liu, N.-W., L. Zhu, and W.-W. Choi, "A differential-fed microstrip patch antenna with bandwidth enhancement under operation of TM 10 and TM 30 modes," *IEEE Transactions on Antennas and Propagation*, Vol. 65, 1607–1614, 2017.
13. Liu, J. and Q. Xue, "Broadband long rectangular patch antenna with high gain and vertical polarization," *IEEE Transactions on Antennas and Propagation*, Vol. 61, 539–546, 2013.
14. Ding, C. and K.-M. Luk, "Low-profile magneto-electric dipole antenna," *IEEE Antennas and Wireless Propagation Letters*, Vol. 15, 1642–1644, 2016.

15. Li, M. and K.-M. Luk, "A differential-fed UWB antenna element with unidirectional radiation," *IEEE Transactions on Antennas and Propagation*, Vol. 64, 3651–3656, 2016.
16. Mosallaei, H. and K. Sarabandi, "Antenna miniaturization and bandwidth enhancement using a reactive impedance substrate," *IEEE Transactions on Antennas and Propagation*, Vol. 52, 2403–2414, 2004.
17. Kamal, S. and A. A. Chaudhari, "Printed meander line MIMO antenna integrated with air gap, DGS and RIS: A low mutual coupling design for LTE applications," *Progress In Electromagnetics Research*, Vol. 71, 149–159, 2017.
18. Chattopadhyay, S., *Trends in Research on Microstrip Antennas*, 2017.
19. Alkurt, F. O. and M. Karaaslan, "Characterization of tunable electromagnetic band gap material with disordered cavity resonator for X band imaging applications by resistive devices," *Optical and Quantum Electronics*, Vol. 51, No. 8, 279, 2019.
20. Alkurt, F. O. and M. Karaaslan, "Pattern reconfigurable metasurface to improve characteristics of low profile antenna parameters," *International Journal of RF and Microwave Computer-Aided Engineering*, https://doi.org/10.1002/mmce.21790, 2019.
21. Bakır, M., et al., "Metamaterial characterization by applying different boundary conditions on triangular split ring resonator type metamaterials," *International Journal of Numerical Modelling: Electronic Networks, Devices and Fields*, Vol. 30, No. 5, e2188, 2017.
22. Sulyman, A. I., et al., "Radio propagation path loss models for 5G cellular networks in the 28 GHz and 38 GHz millimeter-wave bands," *IEEE Communications Magazine*, Vol. 52, No. 9, 78–86, 2014.
23. Hong, W., et al., "Study and prototyping of practically large-scale mmWave antenna systems for 5G cellular devices," *IEEE Communications Magazine*, Vol. 52, No. 9, 63–69, 2014.
24. Esen, M., et al., "Investigation of electromagnetic and ultraviolet properties of nano-metal-coated textile surfaces," *Applied Nanoscience*, 1–11, 2019.
25. *Agilent Advanced Design System, Santa Rose, CA: Keysight EEsof EDA*.
26. Wadell, B. C., *Transmission Line Design Handbook*, Artech House, 1991.
27. Alley, G. D., "Interdigital capacitors and their application to lumped-element microwave integrated circuits," *IEEE Transactions on Microwave Theory and Techniques*, Vol. 18, No. 12, 1028–1033, 1970.
28. Bahl, I. J., *Lumped Elements for RF and Microwave Circuits*, Artech House, 2003.
29. CST Microwave Studio, LLC, US, Computer Simulation Technology Studio Suite.